

Zero minors of the neutrino mass matrix

E. I. Lashin^{1,2,3*} and N. Chamoun^{1,4†},

¹ The Abdus Salam ICTP, P.O. Box 586, 34100 Trieste, Italy.

² Ain Shams University, Faculty of Science, Cairo 11566, Egypt.

³ Department of physics and Astronomy, College of Science, King Saud University, Riyadh, Saudi Arabia,

⁴ Physics Department, HIAST, P.O.Box 31983, Damascus, Syria.

January 5, 2020

Abstract

We examine the possibility that a certain class of neutrino mass matrices, namely those with two independent vanishing minors in the flavor basis, regardless of being invertible or not, is sufficient to describe current data. We compute generic formulae for the ratios of the neutrino masses and for the Majorana phases. We find that seven textures with two vanishing minors can accommodate the experimental data. We present an estimate of the mass matrix for these patterns. All the possible textures can be dynamically generated through the seesaw mechanism augmented with a discrete Abelian symmetry.

PACS numbers: 14.60.Pq; 11.30.Hv; 14.60.St

1 Introduction

The results of the Super-Kamiokande [1] on the solar neutrino (ν_e) deficit and the atmospheric neutrino (ν_μ) anomaly can be interpreted if attributed to neutrino oscillations, which in turn can naturally occur if neutrinos are massive and lepton flavors are mixed [2]. Massive neutrinos are commonly believed to be Majorana particles, and at low energy scales, the phenomenology of lepton masses and flavor mixing can be formulated in terms of the charged lepton mass matrix M_l and the (effective) neutrino mass matrix M_ν . They totally involve twelve physical parameters: three masses of charged leptons (m_e , m_μ and m_τ), which have precisely been measured [3]; three masses of neutrinos (m_1 , m_2 and m_3), whose relative sizes have been estimated from solar and atmospheric neutrino oscillations [4, 5, 6]; three angles of flavor mixing (θ_x , θ_y and θ_z), whose values have been constrained to an acceptable accuracy also from solar, atmospheric and reactor neutrino oscillations [4, 5, 6, 7]; and three phases of CP violation (two Majorana-type ρ , σ and one Dirac-type δ), which are completely unrestricted by current neutrino data.

One can work in the flavor basis which identifies the flavor eigenstates of the charged leptons with their mass eigenstates, so that M_ν will contain nine free parameters. However, in order to account for the experimental constraints, we need extra assumptions for M_ν . The general idea is to assume that some independent matrix elements of M_ν are actually dependent upon one another, caused by an underlying (broken) flavor symmetry. In particular, this dependence becomes very simple and transparent, if the relevant matrix elements are exactly equal to zero.

*elashin@ictp.it

†nchamoun@ictp.it

In fact, general categories of zero-textures were studied: Out of the twenty possible patterns of M_ν with three independent vanishing entries, none is allowed by current neutrino oscillation data, while of the fifteen possible patterns of M_ν with two independent vanishing entries, there are nine patterns which are found to be compatible with current experimental data (albeit two of them are only marginally allowed [8, 9]). As to the six possible one-zero textures of M_ν , they were studied within a specific model having two heavy right handed neutrinos in [10]. This model leads always to a vanishing mass eigenvalue and there are three textures of M_ν with $m_1 = 0$ and four textures of M_ν with $m_3 = 0$ which are compatible with the current neutrino data .

In this paper, we adopt a new texture of two independent vanishing minors in the mass matrix M_ν . Since a zero-element can be viewed as a zero-determinant of a 1×1 sub-matrix, then the pattern with vanishing minors (which are determinants of 2×2 sub-matrices) can be viewed as a generalization of the zero-textures belonging to the same category of matrices with vanishing sub-determinants. In fact, a zero minor in M_ν can be related to a zero entry in the Majorana mass matrix of the right handed singlet neutrinos M_R in the canonical see-saw mechanism:

$$M_\nu = M_D M_R^{-1} M_D^T, \quad (1)$$

where M_D is the Dirac neutrino mass matrix. It was argued [11] that the zeros of M_R have a deeper theoretical meaning than the texture zero of M_ν and that if M_D is diagonal then texture zeros of M_R are reflected in M_ν as zero minors. To keep M_D diagonal and to maintain the form of the studied pattern of M_ν , a suitable family symmetry (A_4) was introduced in [12].

The work of [13] investigated viable textures with two zeros in the inverted neutrino mass matrix M_ν^{-1} and, using abelian symmetries with one or two heavy scalar singlets, realizations of these textures were constructed. Our work assuming two vanishing minors is somehow different from the work of [13] in the following three points:

- It is true that a vanishing cofactor of the neutrino mass matrix implies a zero in the inverse neutrino mass matrix, but the equivalence comes when the inverse exists. Differently from [13], we did not assume that the neutrino mass matrix is invertible, and in some cases in our work we could make one of the masses m_1 m_2 or m_3 exactly equal to zero.
- The motivation for studying the texture of vanishing minors is somehow different from that for studying the zero texture in the inverse mass matrix, in the sense that we are generalizing the zero texture in a non trivial way, regardless of its relation to zero textures in other matrices. In [14], textures containing two independent traceless 2×2 sub-matrices were studied, while here we study textures of two independent ‘determinant-less’ 2×2 sub-matrices.
- The phenomenological analysis in this paper contains different details from that of [13]. The strategy we followed consisted of the fact that putting two minors equal to zero gives us four real conditions, so with plausible values for five given input data parameters (the three mixing angles θ_x , θ_y and θ_z , and the Dirac CP-violating phase δ , and one input taken to be the solar neutrino mass-squared difference Δm_{sol}^2), one should be able to test the validity of the model to fit the other data. We have spanned almost the whole parameter space in order to find phenomenologically acceptable regions. Whereas in [14], eight textures out of the possible fifteen textures of vanishing two-subtraces were shown to be allowed by experimental data, here we find that seven zero-minor textures are able to accommodate the current data, and five others can marginally do so, while three cases fail completely.

For acceptable values of the input parameters, we give an order of magnitude to the neutrino mass matrix, and find that six of the two-zeroes textures can be reproduced. Of these latter six cases, four

patterns, already studied in [9], are allowed phenomenologically. This classification of patterns agrees well with the work of [13].

The plan of the paper is as follows: in section 2, we review the standard notation for the three-flavor neutrino oscillations and its relation to the experimental constraints. In section 3, we present the texture of M_ν with two independent vanishing minors and compute the expressions of the two neutrino mass ratios and the Majorana phases. We classify the patterns and present the results and the phenomenological analysis of each case in sections 4–7. The symmetry realization of all models is presented in section 8. We end up by conclusions in section 9.

2 Standard notation

In the flavor basis where the charged lepton mass matrix is diagonal, the symmetric neutrino mass matrix M_ν can be diagonalized by a unitary transformation,

$$V^\dagger M_\nu V^* = \begin{pmatrix} m_1 & 0 & 0 \\ 0 & m_2 & 0 \\ 0 & 0 & m_3 \end{pmatrix}, \quad (2)$$

with m_i (for $i = 1, 2, 3$) real and positive, while the lepton flavor mixing matrix V can be written as a product of a Dirac-type flavor mixing matrix U (consisting of three mixing angles and one CP-violating phase) and a diagonal phase matrix P (consisting of two nontrivial Majorana phases): $V = UP$ where $P = \text{diag}(e^{i\rho}, e^{i\sigma}, 1)$. With

$$\lambda_1 = m_1 e^{2i\rho}, \quad \lambda_2 = m_2 e^{2i\sigma}, \quad \lambda_3 = m_3, \quad (3)$$

we may rewrite M_ν as

$$M_\nu = U \begin{pmatrix} \lambda_1 & 0 & 0 \\ 0 & \lambda_2 & 0 \\ 0 & 0 & \lambda_3 \end{pmatrix} U^T. \quad (4)$$

As to the matrix U , and taking the indices $(1, 2, 3)$ to refer to the flavors (e, μ, τ) respectively, it can be parameterized as [9]:

$$U = \begin{pmatrix} c_x c_z & s_x c_z & s_z \\ -c_x s_y s_z - s_x c_y e^{-i\delta} & -s_x s_y s_z + c_x c_y e^{-i\delta} & s_y c_z \\ -c_x c_y s_z + s_x s_y e^{-i\delta} & -s_x c_y s_z - c_x s_y e^{-i\delta} & c_y c_z \end{pmatrix}, \quad (5)$$

where $s_x \equiv \sin \theta_x$, $c_x \equiv \cos \theta_x$ (we will use later also the notation t_x for $\tan x$), and so on. A remarkable merit of this parametrization is that its three mixing angles $(\theta_x, \theta_y, \theta_z)$ are directly related to the mixing angles of solar, atmospheric and CHOOZ reactor neutrino oscillations:

$$\theta_x \approx \theta_{\text{sol}}, \quad \theta_y \approx \theta_{\text{atm}}, \quad \theta_z \approx \theta_{\text{chz}}. \quad (6)$$

Also we have,

$$\Delta m_{\text{sol}}^2 = |\Delta m_{21}^2| = |m_2^2 - m_1^2|, \quad \Delta m_{\text{atm}}^2 = |\Delta m_{32}^2| = |m_3^2 - m_2^2|, \quad (7)$$

and the hierarchy of solar and atmospheric neutrino mass-squared differences is characterized by the parameter:

$$R_\nu \equiv \left| \frac{m_2^2 - m_1^2}{m_3^2 - m_2^2} \right| \approx \frac{\Delta m_{\text{sol}}^2}{\Delta m_{\text{atm}}^2} \ll 1. \quad (8)$$

Reactor nuclear experiments on beta-decay kinematics and neutrinoless double-beta decay put constraints on the neutrino mass scales characterized by the following parameters: the effective electron-neutrino mass

$$\langle m \rangle_e = \sqrt{\sum_{i=1}^3 (|V_{ei}|^2 m_i^2)} , \quad (9)$$

and the effective Majorana mass term $\langle m \rangle_{ee}$ given by

$$\langle m \rangle_{ee} = |m_1 V_{e1}^2 + m_2 V_{e2}^2 + m_3 V_{e3}^2| . \quad (10)$$

Also, cosmological observations put an upper bound on the ‘sum’ parameter Σ which is:

$$\Sigma = \sum_{i=1}^3 m_i . \quad (11)$$

A recent global analysis of neutrino experimental data ([15] and references therein), gives the following estimates, at the confidence level of 95%, for the above parameters:

$$\begin{aligned} \Delta m_{\text{atm}}^2 &= (2.4_{-0.6}^{+0.5}) \times 10^{-3} \text{ eV}^2, \\ \Delta m_{\text{sol}}^2 &= (7.92 \pm 0.7) \times 10^{-5} \text{ eV}^2, \\ \sin^2 \theta_{\text{atm}} = (0.44_{-0.01}^{+0.18}) &\longleftrightarrow \theta_y = (41.55_{-5.6}^{+10.4}) \text{ degree}, \\ \sin^2 \theta_{\text{sol}} = (0.314_{-0.047}^{+0.057}) &\longleftrightarrow \theta_x = (34.08_{-3}^{+3.4}) \text{ degree}, \\ \sin^2 \theta_{\text{chz}} = (0.9_{-0.9}^{+2.3}) \times 10^{-2} &\longleftrightarrow \theta_z = (5.44_{-5}^{+5}) \text{ degree}, \\ \langle m \rangle_e &< 1.8 \text{ eV}, \\ \Sigma &< 1.4 \text{ eV}, \\ \langle m \rangle_{ee} &= (0.58_{-0.16}^{+0.22}) \text{ eV}. \end{aligned} \quad (12)$$

In particular, the bounds on R_ν put very stringent conditions on any model required to fit the data:

$$R_\nu = (0.033_{-0.008}^{+0.016}) . \quad (13)$$

Note that the lower bound on $\langle m \rangle_{ee}$ disappears if the neutrinoless double-beta decay does not exist.

3 Neutrino mass matrices with two vanishing minors

As M_ν is 3×3 symmetric matrix, it totally has 6 independent complex entries, and thus it has 6 independent minors. We will denote by C_{ij} the minor corresponding to the ij^{th} element (i.e. the determinant of the sub-matrix obtained by deleting the i^{th} row and the j^{th} column of M_ν). Hence, we have 15 possibilities of having vanishing two minors. If two minors vanish, we have

$$M_{\nu ab} M_{\nu cd} - M_{\nu ij} M_{\nu mn} = 0, \quad (14)$$

$$M_{\nu a'b'} M_{\nu c'd'} - M_{\nu i'j'} M_{\nu m'n'} = 0, \quad (15)$$

then we have

$$\sum_{l,k=1}^3 (U_{al} U_{bl} U_{ck} U_{dk} - U_{il} U_{jl} U_{mk} U_{nk}) \lambda_l \lambda_k = 0, \quad (16)$$

and a similar equation with $(abcdijmn)$ replaced by their ‘primes’. We get

$$\frac{\lambda_1}{\lambda_3} = \frac{A_2 B_1 - A_1 B_2}{B_2 A_3 - B_3 A_2}, \quad (17)$$

$$\frac{\lambda_2}{\lambda_3} = \frac{A_2 B_1 - A_1 B_2}{A_1 B_3 - A_3 B_1}, \quad (18)$$

where

$$A_h = (U_{al}U_{bl}U_{ck}U_{dk} - U_{il}U_{jl}U_{mk}U_{nk}) + (l \leftrightarrow k), \quad (19)$$

$$B_h = (U_{a'l}U_{b'l}U_{c'k}U_{d'k} - U_{i'l}U_{j'l}U_{m'k}U_{n'k}) + (l \leftrightarrow k), \quad (20)$$

with (h, l, k) are a cyclic permutation of $(1, 2, 3)$.

In this way, with the input of four parameters determining the matrix U (the three mixing angles θ_x , θ_y , θ_z and the Dirac phase δ), we are able to predict the relative magnitude of the three neutrino masses and the values of the two Majorana phases from the relations:

$$\frac{m_i}{m_3} = \left| \frac{\lambda_i}{\lambda_3} \right| \text{ for } i = 1, 2, \quad (21)$$

and

$$\rho = \frac{1}{2} \arg \left(\frac{\lambda_1}{\lambda_3} \right), \quad (22)$$

$$\sigma = \frac{1}{2} \arg \left(\frac{\lambda_2}{\lambda_3} \right). \quad (23)$$

We can examine now whether or not the chosen texture of M_ν is empirically acceptable by computing the magnitude of the parameter R_ν which should be in the order of 10^{-2} (equation 13). With some plausible values of the input parameters, and taking Δm_{sol}^2 to be its ‘central’ allowable experimental value, one can reconstruct the mass matrix and test whether or not the other experimental constraints are respected.

We found that the resulting mass patterns could be classified into two categories:

- Normal hierarchy: characterized by $m_1 \sim m_2 < m_3$ and is denoted by **N**.
- Inverted hierarchy: characterized by $m_1 \sim m_2 > m_3$ and is denoted by **I**.

In addition, there are three patterns which are not suitable to accommodate the data.

The possibility of having non-invertible mass matrix is examined for each pattern. The viable non-invertible mass matrices are characterized by vanishing one of the masses (m_1, m_2 , and m_3), as compatibility with the data prevents the simultaneous vanishing of two masses. The conditions and relations satisfied for each possibility are as follows:

- The vanishing of m_1 implies that $A_1 = B_1 = 0$ and the mass spectrum of m_2 and m_3 takes the values $\sqrt{\Delta m_{\text{sol}}^2}$ and $\sqrt{\Delta m_{\text{sol}}^2 + \Delta m_{\text{atm}}^2}$ respectively.
- The vanishing of m_2 implies that $A_2 = B_2 = 0$ and the mass spectrum of m_1 and m_3 takes the values $\sqrt{\Delta m_{\text{sol}}^2}$ and $\sqrt{\Delta m_{\text{atm}}^2}$ respectively.
- The vanishing of m_3 implies that $A_3 = B_3 = 0$ and the mass spectrum of m_2 and m_1 takes the values $\sqrt{\Delta m_{\text{atm}}^2}$ and $\sqrt{\Delta m_{\text{atm}}^2 \pm \Delta m_{\text{sol}}^2}$ respectively.

4 Results of textures with two vanishing minors

We present now the fifteen patterns corresponding to two vanishing minors, referred to by their corresponding elements, in the neutrino mass matrix M_ν . When the expressions are complicated we only state the analytical leading terms of the expansions in powers of s_z . The numerical estimates, for quick reference, are shown in tables (1,2), where we fixed, when possible, the input parameters $(\theta_x, \theta_y, \theta_z)$ to their ‘experimental’ centered values $(34^\circ, 42^\circ, 5^\circ)$.

5 Normal hierarchy models

Pattern N1: vanishing minors(33,31): We get

$$\begin{aligned}\frac{\lambda_1}{\lambda_3} &= -\frac{s_y}{c_y} \cdot \frac{s_x s_y - c_x c_y s_z e^{-i\delta}}{s_x c_y + c_x s_y s_z e^{i\delta}} e^{2i\delta}, \\ \frac{\lambda_2}{\lambda_3} &= -\frac{s_y}{c_y} \cdot \frac{c_x s_y + s_x c_y s_z e^{-i\delta}}{c_x c_y - s_x s_y s_z e^{i\delta}} e^{2i\delta}.\end{aligned}\tag{24}$$

We have the following analytical approximations:

$$\begin{aligned}\frac{m_1}{m_3} &\approx t_y^2 + O(s_z), \\ \frac{m_2}{m_3} &\approx t_y^2 + O(s_z), \\ R_\nu &\approx \left| \frac{1 + t_x^2 t_y^2 t_{2y} c_\delta s_z}{t_x} \right| + O(s_z^2), \\ \rho &\approx \delta \pm \frac{\pi}{2} + O(s_z), \\ \sigma &\approx \delta \pm \frac{\pi}{2} + O(s_z), \\ \frac{\langle m \rangle_{ee}}{m_3} &\approx t_y^2 + O(s_z), \\ \frac{\langle m \rangle_e}{m_3} &\approx t_y^2 + O(s_z).\end{aligned}\tag{25}$$

In this pattern, we find that in order to match the experimental results, the required values should be around $(\theta_x = 34^\circ, \theta_y = 42^\circ, \delta = 88.3^\circ, \theta_z = 5^\circ)$. For these inputs we obtain $m_1/m_3 = 0.8073998611$, $m_2/m_3 = 0.8141569633$, $\rho = 179.093^\circ$, $\sigma = 177.953^\circ$ and $R_\nu = 0.325$. The mass m_3 fitted from the observed Δm_{sol}^2 is then $m_3 = 0.085$ eV, whereas the values for the other remaining parameters would be $\Delta m_{\text{atm}}^2 = 2.5 \times 10^{-3}$ eV², $\langle m \rangle_e = 0.069$ eV, $\langle m \rangle_{ee} = 0.069$ eV and $\Sigma = 0.223$ eV.

The numerically estimated mass matrix M_ν is

$$M_\nu = m_3 \begin{pmatrix} 0.810 - 0.0355i & -0.213 \times 10^{-8} + 0.125 \times 10^{-7}i & 0.022 + 0.417 \times 10^{-2}i \\ -0.213 \times 10^{-8} + 0.125 \times 10^{-7}i & -0.99 \times 10^{-8} - 0.202 \times 10^{-8}i & 0.900 + 0.334 \times 10^{-9}i \\ 0.022 + 0.417 \times 10^{-2}i & 0.900 + 0.334 \times 10^{-9}i & 0.187 - 0.491 \times 10^{-3}i \end{pmatrix}\tag{26}$$

Numerically, we find that for the choices $\delta = 88.3^\circ$ and $\theta_z = 5^\circ$, the acceptable region in the parameter space of θ_x, θ_y is quite large (figure1(a), where we marked the points satisfying the R_ν constraint in eq.(13): $0.025 < R_\nu < 0.05$, by a small circle). This clearly indicates that no tuning is required for the mixing angles θ_x and θ_y to assure their consistency with the R_ν -constraint. Furthermore, no consistent solution could be found in the limit where one of the masses vanishes. If we look at the numerical order of magnitude for this case, we see that the mass matrix is a two zero-texture matrix corresponding to

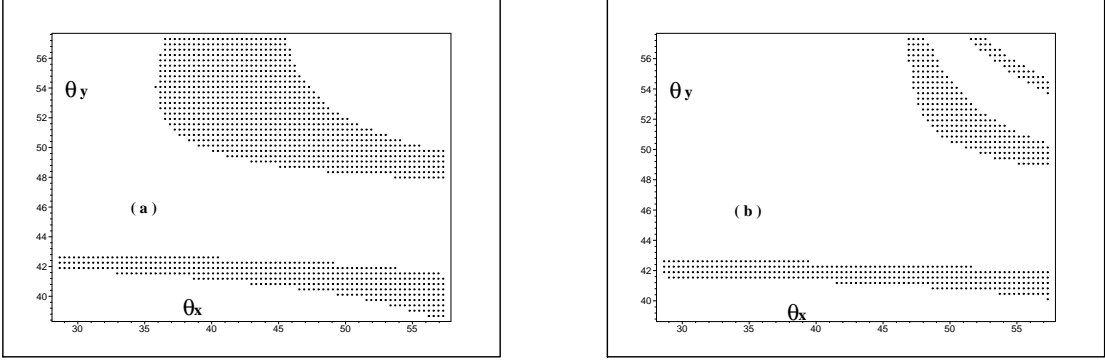


Figure 1: The available θ_x, θ_y parameter space for the two cases **N1** (a) with $\delta = 88.3^\circ$ and **N2** (b) with $\delta = 92^\circ$ respectively. The region whose points marked by small circles represents the set of points (θ_x, θ_y) at which R_ν is constrained by $0.025 < R_\nu < 0.05$. The range from 29° to 57° is spanned for both angles θ_x and θ_y .

the pattern denoted by (B3) in [9], and the analytical expressions given by eqs. 24-25 are identical to the ones there.

Pattern N2: vanishing minors (33,12): We get

$$\begin{aligned} \frac{\lambda_1}{\lambda_3} &= \frac{s_x c_x c_y s_z^2 (1 + s_y^2) e^{-2i\delta} + s_z s_y^3 c_{2x} e^{-i\delta} + s_x c_y c_x s_y^2}{s_z s_y c_y^2 s_x^2 e^{-3i\delta} + [-c_x c_y^3 s_x (1 + s_z^2) + 2 s_x c_y c_x s_z^2] e^{-2i\delta} + s_z c_x^2 s_y^3 e^{-i\delta}}, \\ \frac{\lambda_2}{\lambda_3} &= \frac{-s_x c_y c_x s_z^2 (1 + s_y^2) e^{-2i\delta} - s_y^3 s_z c_{2x} e^{-i\delta} - c_x s_x c_y s_y^2}{s_z s_y c_y^2 c_x^2 e^{-3i\delta} + [-2 s_x c_x c_y s_z^2 + s_x c_x c_y^3 (1 + s_z^2)] e^{-2i\delta} + s_z s_x^2 s_y^3 e^{-i\delta}}. \end{aligned} \quad (27)$$

We have the following analytical approximations:

$$\begin{aligned} \frac{m_1}{m_3} &\approx t_y^2 + O(s_z), \\ \frac{m_2}{m_3} &\approx t_y^2 + O(s_z), \\ R_\nu &\approx \left| \frac{2s_x \cos(\delta) s_y^5}{3c_x s_x^2 c_y s_y^2 - 2c_x s_x^2 c_y s_y^4 - c_x s_x^2 c_y} s_z \right| + O(s_z^2), \\ \rho &\approx \delta \pm \frac{\pi}{2} + O(s_z), \\ \sigma &\approx \delta \pm \frac{\pi}{2} + O(s_z), \\ \frac{\langle m \rangle_{ee}}{m_3} &\approx t_y^2 + O(s_z), \\ \frac{\langle m \rangle_e}{m_3} &\approx t_y^2 + O(s_z). \end{aligned} \quad (28)$$

In this pattern, matching the experimental results, we find that the required input values are $(\theta_x = 34^\circ, \theta_y = 42^\circ, \delta = 92^\circ, \theta_z = 5^\circ)$. For these inputs we obtain $m_1/m_3 = 0.8018004128$, $m_2/m_3 = 0.8090251390$, $\rho = 1.4^\circ$, $\sigma = 2.34^\circ$ and $R_\nu = 0.0336$. The mass m_3 fitted from the observed Δm_{sol}^2 is $m_3 = 0.082$ eV, and then the values for the other remaining parameters are inferred to be $\Delta m_{\text{atm}}^2 = 2.4 \times 10^{-3}$ eV², $\langle m \rangle_e = 0.066$ eV, $\langle m \rangle_{ee} = 0.066$ eV and $\Sigma = 0.215$ eV. The numerically estimated mass matrix M_ν , in this pattern, is

$$M_\nu = m_3 \begin{pmatrix} 0.804 + 0.047i & 0.021 - 0.495 \times 10^{-2}i & 0.441 \times 10^{-2} - 0.107 \times 10^{-2}i \\ 0.021 - 0.495 \times 10^{-2}i & 0.487 \times 10^{-3} - 0.284 \times 10^{-3}i & 0.898 + 0.839 \times 10^{-3}i \\ 0.441 \times 10^{-2} - 0.107 \times 10^{-2} & 0.898 + 0.839 \times 10^{-3}i & 0.191 - 0.629 \times 10^{-3}i \end{pmatrix}. \quad (29)$$

Thus, as in the case **N1**, one can find ‘acceptable’ input parameters and accommodate the data. Again, tuning is not required for the mixing angles θ_x and θ_y in order to assure their consistency with the constraint R_ν in eq. 13 as is evident from figure (1,b). No consistent solution can be found when attaining the limit of one vanishing mass.

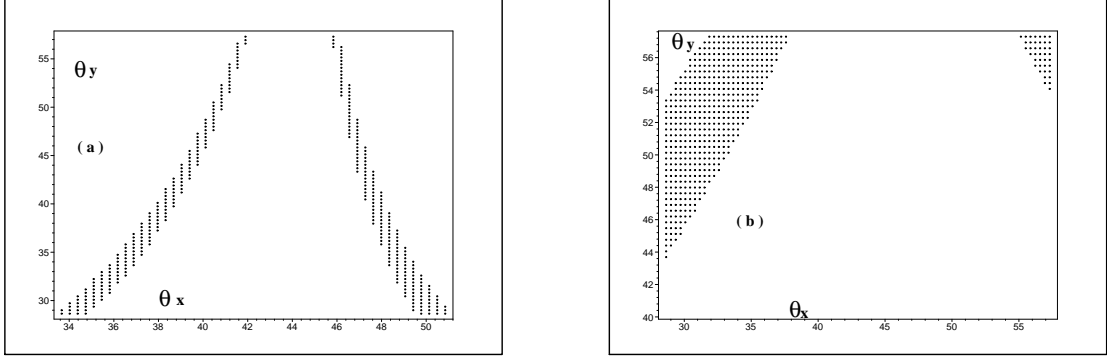


Figure 2: The available θ_x, θ_y parameter space for the two cases **N3** (a) with $\delta = 180^\circ$ and **N4** (b) with $\delta = 0^\circ$ respectively. The region whose points marked by small circles represents the set of points (θ_x, θ_y) at which R_ν is constrained by $0.025 < R_\nu < 0.05$. The range from 29° to 57° is spanned for both angles θ_x and θ_y .

Pattern N3: vanishing minors (33,11): We get

$$\begin{aligned} \frac{\lambda_1}{\lambda_3} &= \frac{c_z^2 c_{2x} s_y^2 + 2 c_z^2 s_x s_y s_z c_x c_y e^{-i\delta}}{c_y^2 s_x^2 c_{2z} e^{-2i\delta} - 2 s_x c_x s_y c_y s_z^3 e^{-i\delta} - c_x^2 s_y^2 s_z^2}, \\ \frac{\lambda_2}{\lambda_3} &= \frac{c_z^2 c_{2x} s_y^2 + 2 c_z^2 s_x s_y s_z c_x c_y e^{-i\delta}}{-c_x^2 c_y^2 c_{2z} e^{-2i\delta} - 2 s_x s_y c_x c_y s_z^3 e^{-i\delta} + s_y^2 s_z^2 s_x^2}. \end{aligned} \quad (30)$$

We have the following analytical approximations:

$$\begin{aligned} \frac{m_1}{m_3} &\approx t_y^2 \frac{c_{2x}}{s_x^2} + O(s_z), \\ \frac{m_2}{m_3} &\approx t_y^2 \frac{c_{2x}}{c_x^2} + O(s_z), \\ R_\nu &\approx \left| \frac{s_y^4 - 8 s_x^6 s_y^4 - 6 s_x^2 s_y^4 + 12 s_x^4 s_y^4}{-s_x^4 + 2 s_x^4 s_y^2 - 4 s_x^6 s_y^2 - 2 s_x^6 s_y^4 - s_x^8 + 2 s_x^8 s_y^2 + 3 s_x^8 s_y^4 + 2 s_x^6} \right| + O(s_z), \\ \rho &\approx \delta \pm \frac{\pi}{2} + O(s_z), \\ \sigma &\approx \delta \pm \frac{\pi}{2} + O(s_z), \\ \frac{\langle m \rangle_{ee}}{m_3} &\approx \frac{4 t_y^2}{t_{2x}^2} + O(s_z), \\ \frac{\langle m \rangle_e}{m_3} &\approx \frac{t_y^2 c_{2x}}{c_x^2 s_x^2} \sqrt{1 - 3 c_x^2 s_x^2} + O(s_z). \end{aligned} \quad (31)$$

In this pattern, we could match the experimental results for the input values ($\theta_x = 39^\circ, \theta_y = 42^\circ, \delta = 180^\circ, \theta_z = 5^\circ$). For these inputs we obtain $m_1/m_3 = 0.2354716727$, $m_2/m_3 = 0.1539511631$, $\rho = 0.335 \times 10^{-7}$ degree, $\sigma = 90^\circ$ and $R_\nu = 0.0325$. The mass m_3 fitted from the observed Δm_{sol}^2 is $m_3 = 0.05$ eV. Then, the values for the other remaining parameters are found to be $\Delta m_{\text{atm}}^2 = 2.4 \times 10^{-3}$ eV², $\langle m \rangle_e = 0.011$ eV, $\langle m \rangle_{ee} = 0.004$ eV and $\Sigma = 0.069$ eV. In this pattern the numerically estimated mass

matrix M_ν is

$$M_\nu = m_3 \begin{pmatrix} 0.088 + 0.194 \times 10^{-10} i & 0.194 + 0.175 \times 10^{-9} i & -0.068 - 0.160 \times 10^{-9} i \\ 0.194 + 0.175 \times 10^{-9} i & 0.428 - 0.842 \times 10^{-10} i & 0.492 + 0.552 \times 10^{-10} i \\ -0.068 - 0.160 \times 10^{-9} i & 0.492 + 0.552 \times 10^{-10} i & 0.565 - 0.308 \times 10^{-10} i \end{pmatrix}. \quad (32)$$

This pattern is marginally accepted, since we could find input parameters satisfying the R_ν constraint in eq. (13), but only for a mixing angle θ_x slightly outside the acceptable region as is clear from the parameter space shown in figure (2.a). A Consistent solution can not be found when reaching the limit of vanishing one mass.

Pattern N4: vanishing minors (33,32): We get

$$\begin{aligned} \frac{\lambda_1}{\lambda_3} &= \frac{s_z}{c_z^2} \left(\frac{s_x s_y}{c_x c_y} e^{i\delta} - s_z \right), \\ \frac{\lambda_2}{\lambda_3} &= -\frac{s_z}{c_z^2} \left(\frac{c_x s_y}{s_x c_y} e^{i\delta} + s_z \right). \end{aligned} \quad (33)$$

This texture implies the absence of neutrinoless double-beta decay:

$$\langle m \rangle_{ee} = 0 \quad (34)$$

We have the following analytical approximations:

$$\begin{aligned} \frac{m_1}{m_3} &\approx t_x t_y s_z + O(s_z^2), \\ \frac{m_2}{m_3} &\approx \frac{t_y}{t_x} s_z + O(s_z^2), \\ R_\nu &\approx \left| \frac{4t_y^2}{s_{2x} t_{2x}} s_z^2 \right| + O(s_z^3), \\ \rho &\approx \frac{\delta}{2} \pm \frac{\pi}{2} + O(s_z), \\ \sigma &\approx \frac{\delta}{2} \pm \frac{\pi}{2} + O(s_z), \\ \frac{\langle m \rangle_e}{m_3} &\approx \frac{1}{c_y} s_z + O(s_z^2). \end{aligned} \quad (35)$$

In this pattern, the required values, to match the experimental results, are $(\theta_x = 34^\circ, \theta_y = 42^\circ, \delta = 0^\circ, \theta_z = 7^\circ)$. For these inputs we obtain $m_1/m_3 = 0.060$, $m_2/m_3 = 0.180$, $\rho = 0^\circ$, $\sigma = 90^\circ$ and $R_\nu = 0.0298$. The mass m_3 fitted from the observed Δm_{sol}^2 is $m_3 = 0.052$ eV, and the other values for the remaining parameters are $\Delta m_{\text{atm}}^2 = 2.7 \times 10^{-3}$ eV², $\langle m \rangle_e = 0.009$ eV, $\langle m \rangle_{ee} = 0$ eV and $\Sigma = 0.065$ eV. In this pattern the numerically estimated mass matrix M_ν is

$$M_\nu = m_3 \begin{pmatrix} 0.363 \times 10^{-8} - 0.228 \times 10^{-10} i & -0.90 \times 10^{-9} - 0.234 \times 10^{-10} i & 0.165 + 0.248 \times 10^{-10} i \\ 0.90 \times 10^{-9} - 0.234 \times 10^{-10} i & 0.396 - 0.241 \times 10^{-10} i & 0.543 + 0.255 \times 10^{-10} i \\ 0.165 + 0.248 \times 10^{-10} i & 0.543 + 0.255 \times 10^{-10} i & 0.483 - 0.271 \times 10^{-10} i \end{pmatrix}. \quad (36)$$

Numerically, we find that the estimated mass matrix has a structure of a two-zero texture and that we have here a strong hierarchy $m_1 \ll m_3$. In fact the formulae (33-35) are identical to those of the two-zero texture denoted by (A1) in [9]. There is no required tuning to fit the experimental data as is clear from the parameter space shown in figure (2.b). The pattern is acceptable, but the numerical fitting is not possible for θ_z quite small, and only for θ_z larger than 7° we can accommodate the data. A Consistent solution can not be found when attaining the vanishing one mass limit.

Pattern N5: vanishing minors (33,22): We get

$$\begin{aligned}\frac{\lambda_1}{\lambda_3} &= \frac{-2 c_x s_x s_y c_y s_z^3 e^{-2i\delta} + (-s_z^2 c_{2y} + 2 c_x^2 s_z^2 c_{2y}) e^{-i\delta} - 2 s_x c_x s_y c_y s_z}{c_z^2 c_x (-c_x c_{2y} + 2 s_x c_y s_z s_y e^{-i\delta}) e^{-i\delta}}, \\ \frac{\lambda_2}{\lambda_3} &= \frac{-2 c_x s_x s_y c_y s_z^3 e^{-2i\delta} + (-s_z^2 c_{2y} + 2 c_x^2 s_z^2 c_{2y}) e^{-i\delta} - 2 s_x c_x s_y c_y s_z}{c_z^2 (s_x^2 c_{2y} + 2 s_x c_y s_z c_x s_y e^{-i\delta}) e^{-i\delta}}.\end{aligned}\quad (37)$$

We have the following analytical approximations:

$$\begin{aligned}\frac{m_1}{m_3} &\approx t_x t_{2y} s_z + O(s_z^2), \\ \frac{m_2}{m_3} &\approx t_x^{-1} t_{2y} s_z + O(s_z^2), \\ R_\nu &\approx \left| \frac{4 t_{2y}^2 s_z^2}{s_{2x} t_{2x}} \right| + O(s_z^3), \\ \rho &\approx \frac{\delta}{2} \pm \frac{\pi}{2} + O(s_z), \\ \sigma &\approx \frac{\delta}{2} \pm \frac{\pi}{2} + O(s_z), \\ \frac{\langle m \rangle_{ee}}{m_3} &\approx \frac{1}{c_{2y}^2} s_z^2 + O(s_z^3), \\ \frac{\langle m \rangle_e}{m_3} &\approx \frac{1}{c_{2y}} s_z + O(s_z^2).\end{aligned}\quad (38)$$

In this pattern, to match the experimental results, the required values are $(\theta_x = 34^\circ, \theta_y = 42^\circ, \delta = 59.3^\circ, \theta_z = 5^\circ)$. For these inputs we obtain $m_1/m_3 = 0.6495617787$, $m_2/m_3 = 0.6335585224$, $\rho = 12.67^\circ$, $\sigma = 136.14^\circ$ and $R_\nu = 0.034$. The mass m_3 fitted from the observed Δm_{sol}^2 is $m_3 = 0.062$ eV. Then the derived values for the other remaining parameters are $\Delta m_{\text{atm}}^2 = 2.2 \times 10^{-3}$ eV², $\langle m \rangle_e = 0.040$ eV, $\langle m \rangle_{ee} = 0.026$ eV and $\Sigma = 0.142$ eV. In this pattern the numerically estimated mass matrix M_ν is

$$M_\nu = m_3 \begin{pmatrix} 0.416 - 0.686 \times 10^{-2} i & -0.333 + 0.657 \times 10^{-2} i & 0.369 - 0.511 \times 10^{-2} i \\ -0.333 + 0.657 \times 10^{-2} i & 0.267 - 0.613 \times 10^{-2} i & 0.699 + 0.474 \times 10^{-2} i \\ 0.369 - 0.511 \times 10^{-2} i & 0.699 + 0.474 \times 10^{-2} i & 0.327 - 0.367 \times 10^{-2} i \end{pmatrix}. \quad (39)$$

In this pattern, the angle θ_y is to be around 42° for a reasonable choice of θ_x as can be seen from Fig. (3.(a)). A Consistent solution could not be found in the limit where one of the masses vanishes.

Pattern N6: vanishing minors (11,32): We get

$$\begin{aligned}\frac{\lambda_1}{\lambda_3} &= \frac{c_z^2 s_x c_x c_{2y} s_z e^{-i\delta} + c_z^2 c_y s_y c_{2x}}{-c_y s_y s_x^2 c_{2z} e^{-2i\delta} - c_x s_x c_{2y} s_z^3 e^{-i\delta} - c_x^2 s_z^2 s_y c_y}, \\ \frac{\lambda_2}{\lambda_3} &= \frac{c_z^2 s_x c_x c_{2y} s_z e^{-i\delta} + c_z^2 c_y s_y c_{2x}}{c_x^2 c_y s_y c_{2z} e^{-2i\delta} - c_x s_x c_{2y} s_z^3 e^{-i\delta} + c_y s_y s_x^2 s_z^2}.\end{aligned}\quad (40)$$

We have the following analytical approximations:

$$\begin{aligned}\frac{m_1}{m_3} &\approx \frac{c_{2x}}{s_x^2} + O(s_z), \\ \frac{m_2}{m_3} &\approx \frac{c_{2x}}{c_x^2} + O(s_z),\end{aligned}$$

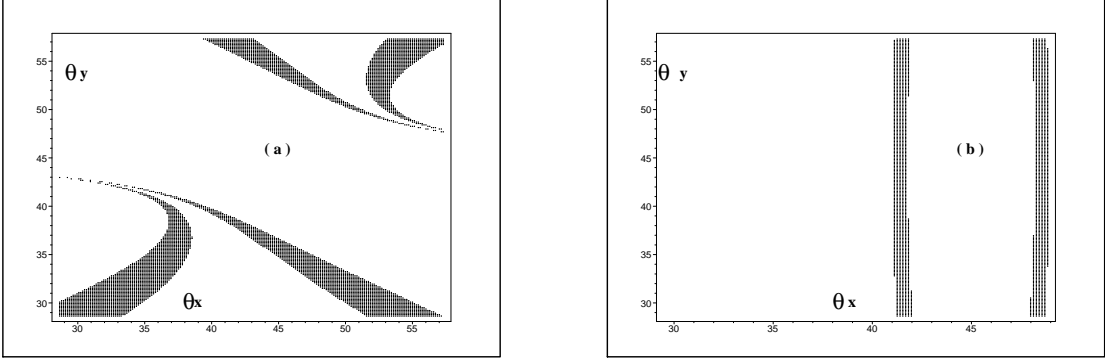


Figure 3: The available θ_x, θ_y parameter space for the two cases **N5** (a) with $\delta = 59.3^\circ$ and **N6** (b) with $\delta = 90^\circ$ respectively. The region whose points marked by small circles represents the set of points (θ_x, θ_y) at which R_ν is constrained by $0.025 < R_\nu < 0.05$. The range from 29° to 57° is spanned for both angles θ_x and θ_y .

$$\begin{aligned}
R_\nu &\approx \left| \frac{1 - 6s_x^2 + 12s_x^4 - 8s_x^6}{3s_x^8 - 2s_x^6} \right| + O(s_z), \\
\rho &\approx \delta \pm \frac{\pi}{2} + O(s_z), \\
\sigma &\approx \delta \pm \frac{\pi}{2} + O(s_z), \\
\frac{\langle m \rangle_{ee}}{m_3} &\approx \frac{4}{t_{2x}^2} + O(s_z), \\
\frac{\langle m \rangle_e}{m_3} &\approx \frac{4}{t_{2x}^2} \sqrt{1 - 3c_x^2 s_x^2} + O(s_z).
\end{aligned} \tag{41}$$

In this pattern, we found the input values $(\theta_x = 41.5^\circ, \theta_y = 42^\circ, \delta = 90^\circ, \theta_z = 5^\circ)$ matching the experimental results. For these inputs we obtain $m_1/m_3 = 0.2832751345$, $m_2/m_3 = 0.2208790064$, $\rho = 177.86^\circ$, $\sigma = 87.87^\circ$ and $R_\nu = 0.033$. The mass m_3 fitted from the observed Δm_{sol}^2 is $m_3 = 0.050$ eV. Then the inferred values for the other remaining parameters are $\Delta m_{\text{atm}}^2 = 2.3 \times 10^{-3}$ eV², $\langle m \rangle_e = 0.014$ eV, $\langle m \rangle_{ee} = 0.003$ eV and $\Sigma = 0.075$ eV. In this model, θ_x turns out to be slightly out of the allowed range and constrained around 41° for any reasonable choice of θ_y , as is clear from the parameter space in Fig. (3(b)). In this pattern the numerically estimated mass matrix M_ν is

$$M_\nu = m_3 \begin{pmatrix} 0.069 - 0.461 \times 10^{-2} i & 0.068 + 0.185 i & 0.048 - 0.166 i \\ 0.068 + 0.185 i & 0.443 - 0.022 i & 0.494 - 0.233 \times 10^{-2} i \\ 0.048 - 0.166 i & 0.494 - 0.233 \times 10^{-2} i & 0.550 + 0.022 i \end{pmatrix}. \tag{42}$$

Numerically, the pattern does not represent an acceptable model since θ_x is beyond its allowed bounds. We found also that the model did not single out any particular value for δ . Furthermore, there does not exist a consistent solution in the limit of vanishing one mass.

Pattern N7: vanishing minors (11,22): We get

$$\begin{aligned}
\frac{\lambda_1}{\lambda_3} &= \frac{c_z^2 c_y (-c_y c_{2x} + 2s_x c_x s_y s_z e^{-i\delta})}{-c_{2z} s_y^2 s_x^2 e^{-2i\delta} + 2s_x c_x s_y c_y s_z c_{2z} e^{-i\delta} + c_x^2 c_y^2 s_z^2}, \\
\frac{\lambda_2}{\lambda_3} &= \frac{c_z^2 c_y (-c_y c_{2x} + 2s_x c_x s_y s_z e^{-i\delta})}{c_x^2 s_y^2 c_{2z} e^{-2i\delta} - 2s_x s_y c_x c_y s_z^3 e^{-i\delta} - c_y^2 s_z^2 s_x^2}.
\end{aligned} \tag{43}$$

We have the following analytical approximations:

$$\begin{aligned}
\frac{m_1}{m_3} &\approx \frac{c_{2x}}{s_x^2 t_y^2} + O(s_z), \\
\frac{m_2}{m_3} &\approx \frac{c_{2x}}{c_x^2 t_y^2} + O(s_z), \\
R_\nu &\approx \left| \frac{c_y^4 (8c_x^6 - 12c_x^4 + 6c_x^2 - 1)}{2c_y^2 c_x^4 + 2c_y^2 c_x^8 - 4c_x^6 c_y^2 - c_x^4 - c_x^8 + 2c_x^6 + 12c_x^4 c_y^4 + 3c_x^8 c_y^4 - 10c_x^6 c_y^4 - 6c_y^4 c_x^2 + c_y^4} \right| + O(s_z), \\
\rho &\approx \delta \pm \frac{\pi}{2} + O(s_z), \\
\sigma &\approx \delta \pm \frac{\pi}{2} + O(s_z), \\
\frac{\langle m \rangle_{ee}}{m_3} &\approx \frac{4}{t_y^2 t_{2x}^2} + O(s_z), \\
\frac{\langle m \rangle_e}{m_3} &\approx \frac{4\sqrt{1 - 3c_x^2 s_x^2}}{t_y^2 t_{2x} s_{2x}} + O(s_z).
\end{aligned} \tag{44}$$

In this pattern, to match the experimental results, the required values are $(\theta_x = 38.5^\circ, \theta_y = 50^\circ, \delta = 0^\circ, \theta_z = 5^\circ)$. For these inputs we obtain $m_1/m_3 = 0.2281999498$, $m_2/m_3 = 0.1439756802$, $\rho = 0^\circ$, $\sigma = 90^\circ$ and $R_\nu = 0.032$. The mass m_3 fitted from the observed Δm_{sol}^2 is $m_3 = 0.050$ eV. Then the derived values for the other remaining parameters are $\Delta m_{\text{atm}}^2 = 2.4 \times 10^{-3}$ eV², $\langle m \rangle_e = 0.011$ eV, $\langle m \rangle_{ee} = 0.005$ eV and $\Sigma = 0.069$ eV. In this pattern the numerically estimated mass matrix M_ν is

$$M_\nu = m_3 \begin{pmatrix} 0.091 - 0.227 \times 10^{-10} i & -0.055 - 0.169 \times 10^{-10} i & 0.189 + 0.232 \times 10^{-10} i \\ -0.055 - 0.169 \times 10^{-10} i & 0.598 - 0.126 \times 10^{-10} i & 0.486 + 0.173 \times 10^{-10} i \\ 0.189 + 0.232 \times 10^{-10} i & 0.486 + 0.173 \times 10^{-10} i & 0.395 - 0.238 \times 10^{-10} i \end{pmatrix} \tag{45}$$

Numerically, we found a quasi real mass matrix, so CP violation will be hard to detect in this case. We note also that, for $\delta = 0$, the input parameters θ_x, θ_y are constrained to be close to their allowed boundaries in order to fit the data as is clear in Fig. 4(a). A Consistent solution can not be found in the limit of vanishing any mass.

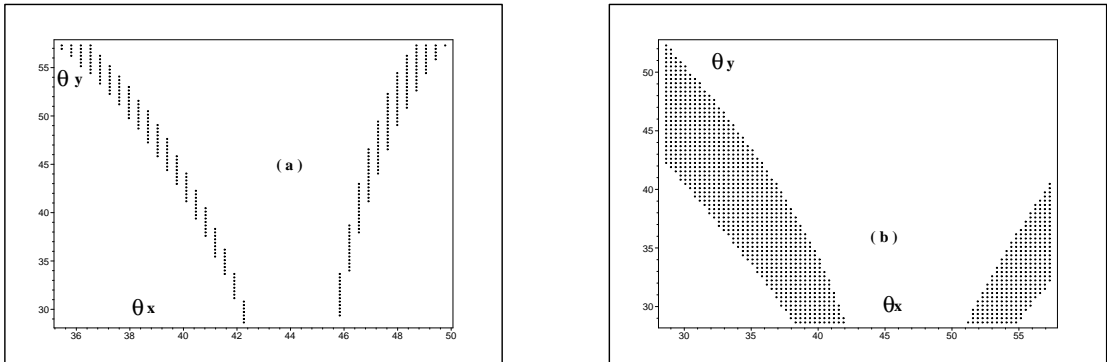


Figure 4: The available θ_x, θ_y parameter space for the two cases **N7** (a) with $\delta = 0^\circ$ and **N8** (b) with $\delta = 180^\circ$ respectively. The region whose points marked by small circles represents the set of points (θ_x, θ_y) at which R_ν is constrained by $0.025 < R_\nu < 0.05$. The range from 29° to 57° is spanned for both angles θ_x and θ_y .

Pattern N8: vanishing minors (22,32): We get

$$\frac{\lambda_1}{\lambda_3} = -\frac{s_z}{c_z^2} \left(\frac{s_x c_y}{c_x s_y} e^{i\delta} + s_z \right),$$

$$\frac{\lambda_2}{\lambda_3} = \frac{s_z}{c_z^2} \left(\frac{c_x c_y}{s_x s_y} e^{i\delta} - s_z \right). \quad (46)$$

This texture implies the absence of neutrinoless double-beta decay:

$$\langle m \rangle_{ee} = 0. \quad (47)$$

We have the following analytical approximations:

$$\begin{aligned} \frac{m_1}{m_3} &\approx \frac{1}{t_x t_y} s_z + O(s_z^2), \\ \frac{m_2}{m_3} &\approx \frac{1}{t_x t_y} s_z + O(s_z^2), \\ R_\nu &\approx \left| \frac{4}{t_y^2 t_{2x} s_{2x}} s_z^2 \right| + O(s_z^3), \\ \rho &\approx \frac{\delta}{2} \pm \frac{\pi}{2} + O(s_z), \\ \sigma &\approx \frac{\delta}{2} \pm \frac{\pi}{2} + O(s_z), \\ \frac{\langle m \rangle_e}{m_3} &\approx \frac{1}{s_y} s_z + O(s_z^2). \end{aligned} \quad (48)$$

In this pattern, no tuning is necessary in order to match the experimental results as it is clear from the parameter space in Fig. 4(b). The required values are $(\theta_x = 34^\circ, \theta_y = 42^\circ, \delta = 180^\circ, \theta_z = 6^\circ)$. For these inputs we obtain $m_1/m_3 = 0.06812223262$, $m_2/m_3 = 0.1850596169$, $\rho = 0.137 \times 10^{-7}$ degree, $\sigma = 90^\circ$ and $R_\nu = 0.031$. The mass m_3 fitted from the observed Δm_{sol}^2 is $m_3 = 0.052$ eV. Then the derived values for the other remaining parameters are $\Delta m_{\text{atm}}^2 = 2.7 \times 10^{-3}$ eV², $\langle m \rangle_e = 0.008$ eV, $\langle m \rangle_{ee} = 0$ eV and $\Sigma = 0.065$ eV. In this pattern the numerically estimated mass matrix M_ν is

$$M_\nu = m_3 \begin{pmatrix} 0.314 \times 10^{-8} - 0.140 \times 10^{-11} i & 0.157 + 0.165 \times 10^{-11} i & -0.72 \times 10^{-9} - 0.129 \times 10^{-11} i \\ 0.157 + 0.165 \times 10^{-11} i & 0.372 + 0.245 \times 10^{-10} i & 0.543 - 0.223 \times 10^{-10} i \\ -0.72 \times 10^{-9} - 0.129 \times 10^{-11} i & 0.543 - 0.223 \times 10^{-10} i & 0.511 + 0.203 \times 10^{-10} i \end{pmatrix} \quad (49)$$

Numerically, we find that the model is consistent with the R_ν constraint, when θ_x and θ_y are fixed to their central values, but only provided that $\theta_z \geq 6^\circ$. This ‘acceptable’ pattern is also a two-zero texture, and the formulae (46-48) are identical with the corresponding expressions in the two-zero texture denoted by (A2) in [9]. We note also that the mass matrix is approximately real with no CP violation. A Consistent solution can not be found in the limit of one mass vanishing.

6 Inverted hierarchy models

Pattern I1: vanishing minors (22,12): We get

$$\begin{aligned} \frac{\lambda_1}{\lambda_3} &= -\frac{c_y}{s_y} \cdot \frac{s_x c_y + c_x s_y s_z e^{-i\delta}}{s_x s_y - c_x c_y s_z e^{i\delta}} e^{2i\delta}, \\ \frac{\lambda_2}{\lambda_3} &= -\frac{c_y}{s_y} \cdot \frac{c_x c_y - s_x s_y s_z e^{-i\delta}}{c_x s_y + s_x c_y s_z e^{i\delta}} e^{2i\delta}. \end{aligned} \quad (50)$$

We have the following analytical approximations:

$$\frac{m_1}{m_3} \approx \frac{1}{t_y^2} + O(s_z),$$

$$\begin{aligned}
\frac{m_2}{m_3} &\approx \frac{1}{t_y^2} + O(s_z), \\
R_\nu &\approx \left| \frac{1+t_x^2}{t_x t_y^2} t_{2y} c_\delta s_z \right| + O(s_z^2), \\
\rho &\approx \delta \pm \frac{\pi}{2} + O(s_z), \\
\sigma &\approx \delta \pm \frac{\pi}{2} + O(s_z), \\
\frac{\langle m \rangle_{ee}}{m_3} &\approx \frac{1}{t_y^2} + O(s_z), \\
\frac{\langle m \rangle_e}{m_3} &\approx \frac{1}{t_y^2} + O(s_z).
\end{aligned} \tag{51}$$

In this pattern, no need for tuning to match the experimental results as it is clear from the parameter space in Fig. 5(a). The required values are $(\theta_x = 34^\circ, \theta_y = 42^\circ, \delta = 90.4^\circ, \theta_z = 5^\circ)$. For these inputs we obtain $m_1/m_3 = 1.226998357$, $m_2/m_3 = 1.233576775$, $\rho = 1.16^\circ$, $\sigma = 0.05^\circ$ and $R_\nu = 0.031$. The mass m_3 fitted from the observed Δm_{sol}^2 is $m_3 = 0.07$ eV. Then the derived values for the other remaining parameters are $\Delta m_{\text{atm}}^2 = 2.6 \times 10^{-3}$ eV², $\langle m \rangle_e = 0.086$ eV, $\langle m \rangle_{ee} = 0.086$ eV and $\Sigma = 0.242$ eV. In this pattern the numerically estimated mass matrix M_ν is

$$M_\nu = m_3 \begin{pmatrix} 1.227 + 0.034 i & -0.03 - 0.005 i & 0.66 \times 10^{-9} + 0.38 \times 10^{-9} i \\ -0.03 - 0.005 i & -0.230 + 0.589 \times 10^{-3} i & 1.111 + 0.319 \times 10^{-10} i \\ 0.66 \times 10^{-9} + 0.38 \times 10^{-9} i & 1.111 + 0.319 \times 10^{-10} i & 0.39 \times 10^{-8} - 0.47 \times 10^{-9} i \end{pmatrix} \tag{52}$$

The numerical solution reproduces a two-zero texture, which can accommodate acceptably the data. Also, the formulae (50-51) are the ones corresponding to the two-zero case denoted by (B4) in [9]. A Consistent solution could not be found when attaining the limit of vanishing any of the masses.

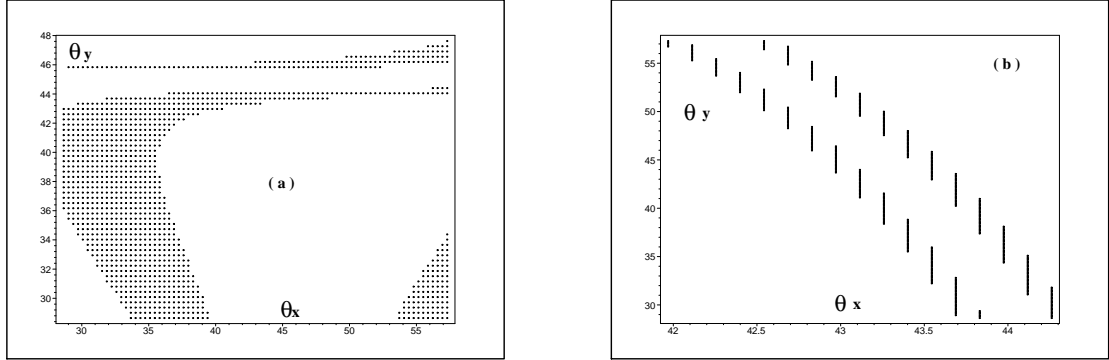


Figure 5: The available θ_x, θ_y parameter space for the two cases **I1** (a) with $\delta = 90.4^\circ$ and **I2** (b) with $\delta = 45^\circ$ respectively. The region whose points marked by small circles represents the set of points (θ_x, θ_y) at which R_ν is constrained by $0.025 < R_\nu < 0.05$. The range from 29° to 57° is spanned for both angles θ_x and θ_y .

Pattern I2: vanishing minors (31,11): We get

$$\begin{aligned}
\frac{\lambda_1}{\lambda_3} &= -\frac{c_z^2 c_x s_y}{s_z (c_x s_y s_z + s_x c_y e^{-i\delta})}, \\
\frac{\lambda_2}{\lambda_3} &= -\frac{s_x c_z^2 s_y}{s_z (s_x s_y s_z - c_x c_y e^{-i\delta})}.
\end{aligned} \tag{53}$$

We have the following analytical approximations:

$$\begin{aligned}
\frac{m_1}{m_3} &\approx \frac{t_y}{t_x} s_z^{-1} + O(1), \\
\frac{m_2}{m_3} &\approx t_x t_y s_z^{-1} + O(1), \\
R_\nu &\approx \left| \frac{1 - 2s_x^2}{s_x^4} \right| + O(s_z), \\
\rho &\approx \frac{\delta}{2} \pm \frac{\pi}{2} + O(s_z), \\
\sigma &\approx \frac{\delta}{2} \pm \frac{\pi}{2} + O(s_z), \\
\frac{\langle m \rangle_{ee}}{m_3} &\approx \frac{2t_y}{t_{2x}} s_z^{-1} + O(1), \\
\frac{\langle m \rangle_e}{m_3} &\approx \frac{2t_y \sqrt{c_x^6 + s_x^6}}{s_{2x}} s_z^{-1} + O(1).
\end{aligned} \tag{54}$$

In this pattern, the θ_x θ_y parameter space, as shown Fig. 5(b), is too limited such that some sort of fine tuning is required. The angle θ_x exceeds the admissible upper limit, and we could not find allowable values for θ_x which can accommodate the data. The best choice for the mixing angles and Dirac phase are $(\theta_x = 43^\circ, \theta_y = 45^\circ, \delta = 45^\circ, \theta_z = 5^\circ)$. For these inputs we obtain $m_1/m_3 = 11.43169109$, $m_2/m_3 = 11.24467888$, $\rho = 110.73^\circ$, $\sigma = 24.24^\circ$ and $R_\nu = 0.034$. The mass m_3 fitted from the observed Δm_{sol}^2 is $m_3 = 0.004$ eV. Then the derived values for the other remaining parameters are $\Delta m_{\text{atm}}^2 = 2.3 \times 10^{-3}$ eV², $\langle m \rangle_e = 0.049$ eV, $\langle m \rangle_{ee} = 0.005$ eV and $\Sigma = 0.102$ eV. In this pattern the numerically estimated mass matrix M_ν is

$$M_\nu = m_3 \begin{pmatrix} -1.1 - 0.130i & 8.082 + 0.535 \times 10^{-8}i & -7.822 + 0.016i \\ 8.082 + 0.535 \times 10^{-8}i & -0.4 \times 10^{-8} - 0.2 \times 10^{-8}i & 10^{-8} \\ -7.822 + 0.016i & 10^{-8}i & 1.968 - 0.199 \times 10^{-2}i \end{pmatrix} \tag{55}$$

Numerically, this model is similar to a two-zero texture.

A consistent solution, in the non-invertible mass matrix situation, is found only for vanishing m_3 , albeit with zero θ_z . A vanishing θ_z is still consistent with experimental data as shown in eq. (12). In this pattern with vanishing m_3 we have $m_1 = \sqrt{\Delta m_{\text{atm}}^2 \pm \Delta m_{\text{sol}}^2}$ and $m_2 = \sqrt{\Delta m_{\text{atm}}^2}$. As to the parameters $\langle m \rangle_{ee}$ and $\langle m \rangle_e$, we have respectively

$$\begin{aligned}
\langle m \rangle_{ee} &= \sqrt{m_1^2 c_x^4 + m_2^2 s_x^4 + 2m_1 m_2 c_x^2 s_x^2 c_{2\rho-2\sigma}}, \\
\langle m \rangle_e &= \sqrt{m_1^2 c_x^2 + m_2^2 s_x^2}.
\end{aligned} \tag{56}$$

The resulting mass matrix has the following elements, where the missing ones are related by symmetry ($M_\nu = M_\nu^T$),

$$\begin{aligned}
M_{\nu 11} &= (m_1 c_x^2 e^{2i\rho} + m_2 s_x^2 e^{2i\sigma}), \\
M_{\nu 12} &= s_x c_x c_y e^{-i\delta} (-m_1 e^{2i\rho} + m_2 e^{2i\sigma}), \\
M_{\nu 13} &= s_x c_x s_y e^{-i\delta} (m_1 e^{2i\rho} - m_2 e^{2i\sigma}), \\
M_{\nu 22} &= c_y^2 e^{-2i\delta} (m_1 s_x^2 e^{2i\rho} + m_2 c_x^2 e^{2i\sigma}), \\
M_{\nu 23} &= -c_y s_y e^{-2i\delta} (m_1 s_x^2 e^{2i\rho} + m_2 c_x^2 e^{2i\sigma}), \\
M_{\nu 33} &= s_y^2 e^{-2i\delta} (m_1 s_x^2 e^{2i\rho} + m_2 c_x^2 e^{2i\sigma}).
\end{aligned} \tag{57}$$

The mixing angles θ_x and θ_y are constrained by data as given in eq. (12). However, there is no constraint on the phases δ, ρ and σ , thus for such a model there is no definite prediction for these phases. For the

sake of illustration, we present a numerical value for the mass matrix for $\delta = 75^0, \rho = 30^0$ and $\sigma = 30^0$, while θ_x and θ_y take their central value as given in eq. (12),

$$M_\nu = m_1 \begin{pmatrix} 0.497 + 0.862 i & -0.006 + 0.001 i & 0.005 - 0.001 i \\ -0.006 + 0.001 i & 0.106 \times 10^{-9} - 0.546 i & -0.123 \times 10^{-9} + 0.492 i \\ 0.005 - 0.001 i & -0.123 \times 10^{-9} + 0.492 i & 0.909 \times 10^{-10} - 0.443 i \end{pmatrix}. \quad (58)$$

Pattern I3: vanishing minors (22,31): We get

$$\begin{aligned} \frac{\lambda_1}{\lambda_3} &= \frac{-c_x s_y s_x s_z^2 (1 + c_y^2) e^{-2i\delta} + s_z c_y^3 c_{2x} e^{-i\delta} - s_x s_y c_x c_y^2}{s_z c_y s_y^2 s_x^2 e^{-3i\delta} + c_x s_y s_x (c_z^2 + c_y^2 c_z^2 - 2 c_y^2) e^{-2i\delta} + s_z c_y^3 c_x^2 e^{-i\delta}}, \\ \frac{\lambda_2}{\lambda_3} &= \frac{-c_x s_y s_x s_z^2 (1 + c_y^2) e^{-2i\delta} + s_z c_y^3 c_{2x} e^{-i\delta} - s_x s_y c_x c_y^2}{-c_x^2 c_y s_z s_y^2 e^{-3i\delta} + c_x s_y s_x (c_z^2 + c_y^2 c_z^2 - 2 c_y^2) e^{-2i\delta} - s_z c_y^3 s_x^2 e^{-i\delta}}. \end{aligned} \quad (59)$$

We have the following analytical approximations:

$$\begin{aligned} \frac{m_1}{m_3} &\approx \frac{1}{t_y^2} + O(s_z), \\ \frac{m_2}{m_3} &\approx \frac{1}{t_y^2} + O(s_z), \\ R_\nu &\approx \left| \frac{-2 c_\delta c_y^5 s_z}{c_x s_x s_y^3 c_{2y}} \right| + O(s_z^2), \\ \rho &\approx \delta \pm \frac{\pi}{2} + O(s_z), \\ \sigma &\approx \delta \pm \frac{\pi}{2} + O(s_z), \\ \frac{\langle m \rangle_{ee}}{m_3} &\approx \frac{1}{t_y^2} + O(s_z), \\ \frac{\langle m \rangle_e}{m_3} &\approx \frac{1}{t_y^2} + O(s_z). \end{aligned} \quad (60)$$

In this pattern, the angles θ_y , as shown in fig. 6(a), is constraint to be close to 42^0 in order to match the experimental results. The required values are $(\theta_x = 34^0, \theta_y = 42^0, \delta = 90.2^0, \theta_z = 5^0)$. For these inputs we obtain $m_1/m_3 = 1.244190882$, $m_2/m_3 = 1.237374512$, $\rho = 0.22^0$, $\sigma = 1.7^0$ and $R_\nu = 0.032$. The mass m_3 fitted from the observed Δm_{sol}^2 is $m_3 = 0.068$ eV. Then the derived values for the other remaining parameters are $\Delta m_{\text{atm}}^2 = 2.5 \times 10^{-3}$ eV², $\langle m \rangle_e = 0.085$ eV, $\langle m \rangle_{ee} = 0.085$ eV and $\Sigma = 0.238$ eV. In this pattern the numerically estimated mass matrix M_ν is

$$M_\nu = m_3 \begin{pmatrix} 1.240 + 0.029 i & 0.007 + 0.912 \times 10^{-3} i & -0.035 - 0.004 i \\ 0.007 + 0.912 \times 10^{-3} i & -0.238 - 0.466 \times 10^{-3} i & 1.114 + 0.312 \times 10^{-3} i \\ -0.035 - 0.004 i & 1.114 + 0.312 \times 10^{-3} i & 0.975 \times 10^{-3} + 0.214 \times 10^{-3} i \end{pmatrix} \quad (61)$$

This pattern is an accepted model able to accommodate the data with allowed input parameters. A Consistent solution can not be found in the limit of one mass vanishing.

Pattern I4: vanishing minors (11,12): We get

$$\begin{aligned} \frac{\lambda_1}{\lambda_3} &= \frac{c_z^2 c_x c_y}{s_z (-c_x c_y s_z + s_x s_y e^{-i\delta})}, \\ \frac{\lambda_2}{\lambda_3} &= -\frac{s_x c_z^2 c_y}{s_z (s_x c_y s_z + c_x s_y e^{-i\delta})}. \end{aligned} \quad (62)$$

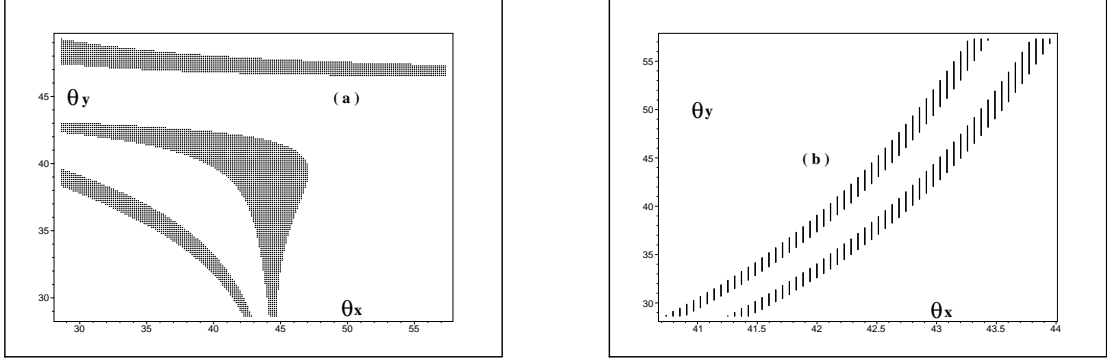


Figure 6: The available θ_x, θ_y parameter space for the two cases **I3** (a) with $\delta = 91.2^\circ$ and **I4** (b) with $\delta = 210^\circ$ respectively. The region whose points marked by small circles represents the set of points (θ_x, θ_y) at which R_ν is constrained by $0.025 < R_\nu < 0.05$. The range from 29° to 57° is spanned for both angles θ_x and θ_y .

We have the following analytical approximations:

$$\begin{aligned}
\frac{m_1}{m_3} &\approx \frac{1}{t_y t_x} s_z^{-1} + O(1), \\
\frac{m_2}{m_3} &\approx \frac{t_x}{t_y} s_z^{-1} + O(1), \\
R_\nu &\approx \left| \frac{c_{2x}}{s_x^4} \right| + O(s_z), \\
\rho &\approx \frac{\delta}{2} \pm \frac{\pi}{2} + O(s_z), \\
\sigma &\approx \frac{\delta}{2} \pm \frac{\pi}{2} + O(s_z), \\
\frac{\langle m \rangle_{ee}}{m_3} &\approx \frac{2}{t_y t_{2x}} s_z^{-1} + O(1), \\
\frac{\langle m \rangle_e}{m_3} &\approx \frac{2\sqrt{1+3c_x^4-3c_x^2}}{t_y s_{2x}} s_z^{-1} + O(1).
\end{aligned} \tag{63}$$

We find here a very restricted allowable region in the parameter space, as shown in fig. 6(b), and only for values of θ_x larger than the experimentally allowed we could satisfy the condition (13). Also, numerically, this pattern is a two-zero texture.

In this pattern to match the experimental results. The acceptable values are $(\theta_x = 42.4^\circ, \theta_y = 42.4^\circ, \delta = 210^\circ, \theta_z = 5^\circ)$. For these inputs we obtain $m_1/m_3 = 12.50828988$, $m_2/m_3 = 12.30251175$, $\rho = 103.63^\circ$, $\sigma = 16.35^\circ$ and $R_\nu = 0.034$. The mass m_3 fitted from the observed Δm_{sol}^2 is $m_3 = 0.004$ eV. Then the derived values for the other remaining parameters are $\Delta m_{\text{atm}}^2 = 2.3 \times 10^{-3}$ eV², $\langle m \rangle_e = 0.049$ eV, $\langle m \rangle_{ee} = 0.005$ eV and $\Sigma = 0.102$ eV. In this pattern the numerically estimated mass matrix M_ν is

$$M_\nu = m_3 \begin{pmatrix} -1.338 - 0.101 i & -8.940 + 0.013 i & 8.440 - 0.324 \times 10^{-9} i \\ -8.940 + 0.013 i & 2.160 - 0.002 i & 0.5 \times 10^{-8} - 0.2 \times 10^{-8} i \\ 8.440 - 0.324 \times 10^{-9} i & 0.5 \times 10^{-8} - 0.2 \times 10^{-8} i & -0.4 \times 10^{-8} + 0.2 \times 10^{-8} i \end{pmatrix} \tag{64}$$

A consistent non-invertible mass matrix solution is only found for vanishing m_3 provided θ_z is equal to zero. The same results are exactly obtained as in the pattern **I2**.

7 Failing cases

There are three patterns which can not account for the neutrino oscillation since they give $m_1 = m_2 = m_3$. They correspond to the cases of vanishing minors: (31,32), (32,12) and (31,12). The ‘latter’ model of vanishing minor (31,12) is somehow exceptional in that it becomes successful when both m_3 and θ_z vanish, with results exactly the same as obtained in patterns **I2** and **I4**.

Model	Minors	Status	θ_x	θ_y	θ_z	δ	R_ν	$\frac{m_1}{m_3}$	$\frac{m_2}{m_3}$	ρ	σ	m_3	Δm_{atm}^2	Σ	$\langle m \rangle_{ee}$	$\langle m \rangle_e$
N1	33, 31	allowed	34	42	5	88.3	0.0325	0.807	0.814	179	178	0.085	0.0025	0.223	0.069	0.069
N2	33, 12	allowed	34	42	5	92	0.0336	0.802	0.809	1.4	2.34	0.082	0.0024	0.215	0.066	0.066
N3	33, 11	disallowed	39	42	5	180	0.0325	0.235	0.154	0	90	0.050	0.0024	0.069	0.004	0.011
N4	33, 32	allowed	34	42	7	0	0.0298	0.060	0.180	0	90	0.052	0.0027	0.065	0	0.009
N5	22, 33	allowed	34	42	5	59.3	0.034	0.650	0.634	12.7	136.14	0.062	0.0022	0.142	0.026	0.040
N6	11, 32	disallowed	41.5	42	5	90	0.033	0.283	0.221	177.9	87.9	0.050	0.0023	0.075	0.003	0.014
N7	22, 11	disallowed	38.5	50	5	0	0.0320	0.228	0.144	0	90	0.050	0.0024	0.069	0.005	0.011
N8	22, 32	allowed	34	42	6	180	0.031	0.068	0.185	~ 0	90	0.052	0.0027	0.065	0	0.008
I1	22, 12	allowed	34	42	5	90.4	0.0310	1.227	1.234	1.16	0.05	0.070	0.0026	0.242	0.086	0.086
I2	31, 11	disallowed	43	45	5	45	0.0334	11.43	11.24	110.7	24.24	0.004	0.0023	0.102	0.005	0.049
I3	22, 31	allowed	34	42	5	90.2	0.032	1.244	1.237	0.22	1.7	0.068	0.0025	0.238	0.085	0.085
I4	11, 12	disallowed	42.4	42.4	5	210	0.034	12.51	12.30	103.6	16.4	0.004	0.0023	0.102	0.005	0.049
	(31, 32)	unaccepted						1	1							
	(31, 12)	unaccepted						1	1							
	(32, 12)	unaccepted						1	1							

Table 1: The 15 patterns for the two-vanishing minors. The minor corresponding to the index (ij) is the determinant of the sub-matrix obtained by deleting the i^{th} line and the j^{th} column. All the angles (masses) are evaluated in degrees (eV). Results for models which are acceptable in the limit of vanishing both m_3 and θ_z are shown in the discussion following each model

8 Symmetry realization

All textures with zero minors discussed in this work can be realized in a simple way in models based on seesaw mechanism with a flavour Abelian symmetry. Zero minors in the non singular neutrino mass matrix (M_ν) are equivalent to zeros in the inverse mass matrix (M_ν^{-1}). This equivalence, however, is valid only for invertible mass matrices. In turn, eq. (1), tells us that, in case of diagonal neutrino Dirac mass matrices, zeros in (M_ν^{-1}) lead to zeros in (M_R).

In order to construct the required leptonic mass matrices, we need three right-handed neutrinos ν_{Rj} , three right-handed charged leptons l_{Rj} and three left-handed lepton doublets $D_{Lj} = (\nu_{Lj}, l_{Lj})^T$, where j is the family index running from 1 to 3. As to the scalar sector, one Higgs doublet, the standard model SM Higgs, and many scalar singlets are required.

The underlying symmetry for building up mass matrices can be an Abelian discrete one as invoked in [13]. Following the same strategy, one can utilize Z_8 for constructing the model **N1** which is characterized by vanishing minors (33, 31), and hence zeros at positions (33, 31) in (M_ν^{-1}). Under the action of Z_8 , leptons of the first family remain invariant, those of the second family change sign, and those of the third get multiplied by $\omega = \exp(\frac{i\pi}{4})$, whereas the SM Higgs doublet remains invariant. These assigned transformations under Z_8 automatically generate diagonal Dirac mass matrices for both charged leptons and neutrinos.

The bilinears $\nu_{Ri}\nu_{Rj}$ under Z_8 , necessary for constructing the Majorana mass for right handed neutrino, transform as

$$\begin{pmatrix} 1 & \omega^4 & \omega \\ \omega^4 & 1 & \omega^5 \\ \omega & \omega^5 & \omega^2 \end{pmatrix}, \quad (65)$$

The (1, 1) and (2, 2) matrix elements of M_R are Z_8 invariant, hence their corresponding mass terms are directly present in the Lagrangian. The (1, 2) matrix element requires the presence of a real scalar singlet (call it χ_{12}) which changes sign under Z_8 . The (2, 3) matrix element is generated by the Yukawa coupling to a complex scalar singlet (call it χ_{23}) which gets multiplied by ω^3 under Z_8 . The other entries of M_R remains zero in the absence of any further scalar singlets. The resulting right-handed Majorana mass matrix can be casted in the form,

$$\begin{pmatrix} \times & \times & 0 \\ \times & \times & \times \\ 0 & \times & 0 \end{pmatrix}, \quad (66)$$

where the cross sign denotes a non-vanishing element.

As to the model **N3**, it can be generated by utilizing Z_4 symmetry. Under the action of Z_4 , leptons of the first and third families get multiplied by i and $-i$ respectively, while those of the second family as well as the SM Higgs remain invariant. As in case **N1**, the assigned transformations guarantee diagonal Dirac mass matrices for both charged leptons and neutrinos, and hence zeros in M_ν^{-1} would appear as zeros in M_R . The bilinears $\nu_{Ri}\nu_{Rj}$ under Z_4 transform as

$$\begin{pmatrix} -1 & i & 1 \\ i & 1 & -i \\ 1 & -i & -1 \end{pmatrix}. \quad (67)$$

The (2, 2) and (1, 3) matrix elements of the symmetric M_R are Z_4 invariant, hence their corresponding mass terms are directly present in the Lagrangian. Only one complex scalar singlet (call it χ_{12}) which gets multiplied by $-i$ is needed together with its complex conjugate (call it χ_{32}) to generate the entries

Model	M_ν		
N₁	m_3	$\begin{bmatrix} 0.810 - 0.0355 i & -0.213 \times 10^{-8} + 0.125 \times 10^{-7} i & 0.022 + 0.417 \times 10^{-2} i \\ -0.213 \times 10^{-8} + 0.125 \times 10^{-7} i & -0.99 \times 10^{-8} - 0.202 \times 10^{-8} i & 0.900 + 0.334 \times 10^{-9} i \\ 0.022 + 0.417 \times 10^{-2} i & 0.900 + 0.334 \times 10^{-9} i & 0.187 - 0.491 \times 10^{-3} i \end{bmatrix}$	
N₂	m_3	$\begin{bmatrix} 0.804 + 0.047 i & 0.021 - 0.495 \times 10^{-2} i & 0.441 \times 10^{-2} - 0.107 \times 10^{-2} i \\ 0.021 - 0.495 \times 10^{-2} i & 0.487 \times 10^{-3} - 0.284 \times 10^{-3} i & 0.898 + 0.839 \times 10^{-3} i \\ 0.441 \times 10^{-2} - 0.107 \times 10^{-2} i & 0.898 + 0.839 \times 10^{-3} i & 0.191 - 0.629 \times 10^{-3} i \end{bmatrix}$	
N₃	m_3	$\begin{bmatrix} 0.088 + 0.194 \times 10^{-10} i & 0.194 + 0.175 \times 10^{-9} i & -0.068 - 0.160 \times 10^{-9} i \\ 0.194 + 0.175 \times 10^{-9} i & 0.428 - 0.842 \times 10^{-10} i & 0.492 + 0.552 \times 10^{-10} i \\ -0.068 - 0.160 \times 10^{-9} i & 0.492 + 0.552 \times 10^{-10} i & 0.565 - 0.308 \times 10^{-10} i \end{bmatrix}$	
N₄	m_3	$\begin{bmatrix} 0.363 \times 10^{-8} - 0.228 \times 10^{-10} i & -0.90 \times 10^{-9} - 0.234 \times 10^{-10} i & 0.165 + 0.248 \times 10^{-10} i \\ 0.90 \times 10^{-9} - 0.234 \times 10^{-10} i & 0.396 - 0.241 \times 10^{-10} i & 0.543 + 0.255 \times 10^{-10} i \\ 0.165 + 0.248 \times 10^{-10} i & 0.543 + 0.255 \times 10^{-10} i & 0.483 - 0.271 \times 10^{-10} i \end{bmatrix}$	
N₅	m_3	$\begin{bmatrix} 0.416 - 0.686 \times 10^{-2} i & -0.333 + 0.657 \times 10^{-2} i & 0.369 - 0.511 \times 10^{-2} i \\ -0.333 + 0.657 \times 10^{-2} i & 0.267 - 0.613 \times 10^{-2} i & 0.699 + 0.474 \times 10^{-2} i \\ 0.369 - 0.511 \times 10^{-2} i & 0.699 + 0.474 \times 10^{-2} i & 0.327 - 0.367 \times 10^{-2} i \end{bmatrix}$	
N₆	m_3	$\begin{bmatrix} 0.069 - 0.461 \times 10^{-2} i & 0.068 + 0.185 i & 0.048 - 0.166 i \\ 0.068 + 0.185 i & 0.443 - 0.022 i & 0.494 - 0.233 \times 10^{-2} i \\ 0.048 - 0.166 i & 0.494 - 0.233 \times 10^{-2} i & 0.550 + 0.022 i \end{bmatrix}$	
N₇	m_3	$\begin{bmatrix} 0.091 - 0.227 \times 10^{-10} i & -0.055 - 0.169 \times 10^{-10} i & 0.189 + 0.232 \times 10^{-10} i \\ -0.055 - 0.169 \times 10^{-10} i & 0.598 - 0.126 \times 10^{-10} i & 0.486 + 0.173 \times 10^{-10} i \\ 0.189 + 0.232 \times 10^{-10} i & 0.486 + 0.173 \times 10^{-10} i & 0.395 - 0.238 \times 10^{-10} i \end{bmatrix}$	
N₈	m_3	$\begin{bmatrix} 0.314 \times 10^{-8} - 0.140 \times 10^{-11} i & 0.157 + 0.165 \times 10^{-11} i & -0.72 \times 10^{-9} - 0.129 \times 10^{-11} i \\ 0.157 + 0.165 \times 10^{-11} i & 0.372 + 0.245 \times 10^{-10} i & 0.543 - 0.223 \times 10^{-10} i \\ -0.72 \times 10^{-9} - 0.129 \times 10^{-11} i & 0.543 - 0.223 \times 10^{-10} i & 0.511 + 0.203 \times 10^{-10} i \end{bmatrix}$	
I₁	m_3	$\begin{bmatrix} 1.227 + 0.034 i & -0.03 - 0.005 i & 0.66 \times 10^{-9} + 0.38 \times 10^{-9} i \\ -0.03 - 0.005 i & -0.230 + 0.589 \times 10^{-3} i & 1.111 + 0.319 \times 10^{-10} i \\ 0.66 \times 10^{-9} + 0.38 \times 10^{-9} i & 1.111 + 0.319 \times 10^{-10} i & 0.39 \times 10^{-8} - 0.47 \times 10^{-9} i \end{bmatrix}$	
I₂	m_3	$\begin{bmatrix} -1.1 - 0.130 i & 8.082 + 0.535 \times 10^{-8} i & -7.822 + 0.016 i \\ 8.082 + 0.535 \times 10^{-8} i & -0.4 \times 10^{-8} - 0.2 \times 10^{-8} i & 10^{-8} \\ -7.822 + 0.016 i & 10^{-8} i & 1.968 - 0.199 \times 10^{-2} i \end{bmatrix}$	
I₃	m_3	$\begin{bmatrix} 1.240 + 0.029 i & 0.007 + 0.912 \times 10^{-3} i & -0.035 - 0.004 i \\ 0.007 + 0.912 \times 10^{-3} i & -0.238 - 0.466 \times 10^{-3} i & 1.114 + 0.312 \times 10^{-3} i \\ -0.035 - 0.004 i & 1.114 + 0.312 \times 10^{-3} i & 0.975 \times 10^{-3} + 0.214 \times 10^{-3} i \end{bmatrix}$	
I₄	m_3	$\begin{bmatrix} -1.338 - 0.101 i & -8.940 + 0.013 i & 8.440 - 0.324 \times 10^{-9} i \\ -8.940 + 0.013 i & 2.160 - 0.002 i & 0.5 \times 10^{-8} - 0.2 \times 10^{-8} i \\ 8.440 - 0.324 \times 10^{-9} i & 0.5 \times 10^{-8} - 0.2 \times 10^{-8} i & -0.4 \times 10^{-8} + 0.2 \times 10^{-8} i \end{bmatrix}$	

Table 2: The mass matrix estimates for the 12 acceptable patterns of the two-vanishing minors. The cases correspond to those of table (1). Results for models which are acceptable in the limit of vanishing both m_3 and θ_z are shown in the discussion following each model.

$(1, 2)$ and $(3, 2)$ in M_R . The resulting mass matrix M_R takes the form

$$\begin{pmatrix} 0 & \times & \times \\ \times & \times & \times \\ \times & \times & 0 \end{pmatrix}, \quad (68)$$

where the cross sign denotes again a non-vanishing element.

Out of fifteen possible models, nine of them **N1**, **N2**, **N4**, **N6**, **N8**, **I1**, **I2**, **I3** and **I4** can be constructed using Z_8 symmetry. The leftover models can be generated using Z_4 symmetry. Symmetry realizations for all models are summarized in Table. (3), where the transformation properties for each lepton family and needed scalar singlets are given for each model. The realization obtained for **N1**, **N2**, **N4**, **N5**, **N8**, **I1** and **I3** models agree with those obtained in [13].

Z_8 Models										
Model	Minors	1_F	2_F	3_F	χ_{11}	χ_{12}	χ_{13}	χ_{22}	χ_{23}	χ_{33}
N1	33, 31	1	-1	ω	absent	-1	absent	absent	ω^3	absent
N2	33, 12	1	-1	ω	absent	absent	ω^7	absent	ω^3	absent
N4	33, 32	1	-1	ω	absent	-1	ω^7	absent	absent	absent
N6	11, 32	ω	-1	1	absent	ω^3	ω^7	absent	absent	absent
N8	22, 32	1	ω	-1	absent	ω^7	-1	absent	absent	absent
I1	22, 12	1	ω	-1	absent	absent	-1	absent	ω^3	absent
I2	31, 11	ω	-1	1	absent	ω^3	absent	absent	ω^4	absent
I3	22, 31	1	ω	-1	absent	ω^7	absent	absent	ω^3	absent
I4	11, 12	ω	-1	1	absent	absent	ω^7	absent	ω^4	absent
Z_4 Models										
N3	33, 11	i	1	$-i$	absent	$-i$	absent	absent	i	absent
N5	22, 33	1	i	$-i$	absent	$-i$	i	absent	absent	absent
N7	22, 11	i	$-i$	1	absent	absent	$-i$	absent	i	absent
	31, 32	i	$-i$	1	-1	absent	absent	-1	absent	absent
	31, 12	1	i	$-i$	absent	absent	absent	-1	absent	-1
	32, 12	i	1	$-i$	-1	absent	absent	absent	absent	-1

Table 3: The symmetry realization for 15 patterns of two-vanishing minors. The index 1_F indicates the lepton first family and so on. The χ_{kj} denotes a scalar singlet which produce the entry (k, j) of the right-handed Majorana mass matrix when acquiring a vev at the see-saw scale. The transformation properties, under the specified group, is listed below each lepton family and needed scalar singlets for each model. ω denotes $\exp(\frac{i\pi}{4})$, while $i = \sqrt{-1}$.

The models **I2**, **I4** and $(31, 12)$ in the limit of vanishing m_3 and θ_z together give a singular mass matrix M_ν . To produce such models of acceptable non-invertible textures within seesaw schemes, M_R can not be singular otherwise the sea-saw mechanism would not work, and hence the only choice is to have a singular Dirac neutrino mass matrix. A simple guess, which by no means excludes other possibilities, is where M_R and M_D have the following forms:

$$M_R = \begin{pmatrix} 0 & \alpha & 0 \\ \alpha & \beta & 0 \\ 0 & 0 & \gamma \end{pmatrix}, \quad M_D = \begin{pmatrix} D & 0 & A \\ 0 & 0 & B \\ 0 & 0 & C \end{pmatrix}, \quad (69)$$

where $A, B, C, D, \alpha, \beta$ and γ are arbitrary parameters. The resulting neutrino mass matrix generated

through seesaw mechanism takes the form,

$$M_\nu = \begin{pmatrix} -\frac{D^2\beta}{\alpha^2} + \frac{A^2}{\gamma} & \frac{AB}{\gamma} & \frac{AC}{\gamma} \\ \frac{AB}{\gamma} & \frac{B^2}{\gamma} & \frac{BC}{\gamma} \\ \frac{AC}{\gamma} & \frac{BC}{\gamma} & \frac{C^2}{\gamma} \end{pmatrix}. \quad (70)$$

This matrix has a zero eigenvalue ($m_3 = 0$) and vanishing minors (31, 11, 12) as required. The symmetry realization for this construction could be done through a generic choice of the group $Z_{12} \times Z_2$ discussed in [16], which may not be the most economic way. The leptonic fields transform as

$$\begin{aligned} l_{R1} &\rightarrow \theta l_{R1}, & \nu_{R1} &\rightarrow \theta \nu_{R1}, & \overline{D}_{L1} &\rightarrow \theta \overline{D}_{L1}, \\ l_{R2} &\rightarrow \theta^2 l_{R2}, & \nu_{R2} &\rightarrow \theta^2 \nu_{R2}, & \overline{D}_{L2} &\rightarrow \theta^3 \overline{D}_{L2}, \\ l_{R3} &\rightarrow \theta^5 l_{R3}, & \nu_{R3} &\rightarrow \theta^5 \nu_{R3}, & \overline{D}_{L3} &\rightarrow \theta^8 \overline{D}_{L3}, \end{aligned} \quad (71)$$

where $\theta = e^{\frac{i\pi}{6}}$. Hence, the bilinears $\overline{D}_{Lj} l_{Rk}$, $\overline{D}_{Lj} \nu_{Rk}$ and $\nu_{Rj} \nu_{Rk}$ transform as

$$\overline{D}_{Lj} l_{Rk} \sim \overline{D}_{Lj} \nu_{Rk} \sim \begin{pmatrix} \theta^2 & \theta^3 & \theta^6 \\ \theta^4 & \theta^5 & \theta^8 \\ \theta^9 & \theta^{10} & \theta \end{pmatrix}, \quad \nu_{Rj} \nu_{Rk} \sim \begin{pmatrix} \theta^2 & \theta^3 & \theta^6 \\ \theta^3 & \theta^4 & \theta^7 \\ \theta^6 & \theta^7 & \theta^{10} \end{pmatrix}. \quad (72)$$

To achieve a diagonal charged lepton mass matrix, only three scalar Higgs doublets are needed which are denoted by Φ_{11} , Φ_{22} and Φ_{33} . Under the action of Z_{12} these scalar doublets get respectively multiplied by θ^{10} , θ^7 and θ^{11} . The Dirac and Majorana neutrino mass matrices in eq. (69) can be achieved equally by introducing scalar Higgs fields with suitable transformation properties, namely four scalar doublets $\tilde{\Phi}_{11}$, $\tilde{\Phi}_{13}$, $\tilde{\Phi}_{23}$, and $\tilde{\Phi}_{33}$, being multiplied respectively by θ^{10} , θ^6 , θ^4 and θ^{11} under Z_{12} , for the Dirac mass term, and three scalar singlets χ_{12} , χ_{22} and χ_{33} , multiplied respectively by θ^9 , θ^8 and θ^2 under Z_{12} , for the Majorana mass term. The $\tilde{\Phi}_{jk}$ scalar Higgs doublet and ν_{Rj} change sign under Z_2 , while all other multiplets remain invariant. It is important to notice that the scalar Higgs doublets take vacuum expectation values (vev) at the electro-weak scale, while scalar singlets acquire vevs at the seesaw scale.

9 Discussion and conclusions

We studied all the possible patterns of Majoran neutrino mass matrices with two independent vanishing minors.

For the possible fifteen cases, we found seven patterns (**N1**, **N2**, **N4**, **N5**, **N8**, **I1** and **I3**) able to accommodate current data, without need to tune the input parameters. Five patterns (**N3**, **N6**, **N7**, **I2** and **I4**) can accommodate marginally the data, in that they can satisfy the constraint (13), but only for a value of the mixing angle θ_x well above its upper accepted bound. Then, in these patterns, one can attribute the experimental value of θ_x to small perturbations on the textures. Three cases predict degeneracy of masses $m_1 = m_2 = m_3$, and thus can not make room for the oscillation phenomena.

Four patterns (**N3**, **N4**, **N7** and **N8**) present, numerically, approximate real mass matrices, and thus it would be difficult to display CP violation phenomena with these patterns. The six cases (**N1**, **N4**, **N8**, **I1**, **I2** and **I4**) appear as ‘two-zero’ textures, and the analytical expressions of the allowed cases (**N1**, **N4**, **N8** and **I1**) of these six cases coincide with the corresponding expressions in the two-zero textures denoted, respectively, by (**B3**, **A1**, **A2** and **B4**) in [9]. The other three two-zero textures allowed by current data, and denoted by (**B1**, **B2** and **C**) in [9], are not reproduced as two-vanishing minors textures. On the other hand, there are three two-vanishing minor textures (**N2**, **N5** and **I3**) which are allowed by data and do not show up as two-zero textures. This classification of patterns coincides exactly with the results of [13]. However, as mentioned in the introduction, the analytical parts of the two approaches

are not completely identical, so that one needs not to assume an invertible neutrino mass matrix in our ‘vanishing minor’ approach.

New results are obtained in case of non-invertible mass matrix which can not be recovered in [13]. Those correspond to the patterns **I2**, **I4** and the one given by vanishing minor (31,12). For these models, we only find a consistent solution when both m_3 and θ_z vanish, a solution that accommodates θ_x and θ_y to be in their acceptable range given in eq. (12), while the phases δ , σ and ρ are not constrained. Peculiarly enough, the three cases have identical mass matrix as given in eq. (57), and thus it would be difficult to distinguish between the three models in this limit of vanishing m_3 and θ_z . An interesting thing about these three models is that they correspond to two-zero textures before taking the limit of vanishing m_3 and θ_z , whereas they cease to be so after taking the limit where they become only characterized by vanishing two minors and the whole determinant.

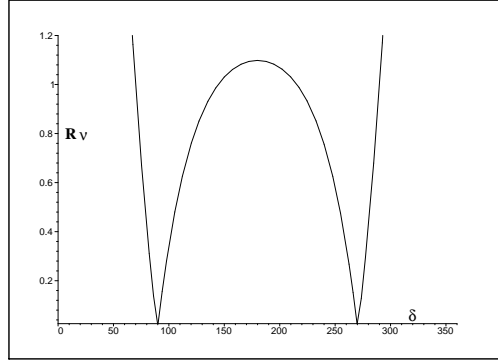


Figure 7: R_ν as a function of δ , for $\theta_x = 34^\circ$, $\theta_y = 42^\circ$, $\theta_z = 5^\circ$, for case **I1**, the values around $\delta = 90^\circ, 270^\circ$ are singled out.

We took, except for the allowed cases **N4**, **N8** textures, the value 5° for the angle θ_z . For these two cases (**N4**, **N8**), the model starts to be consistent with the experimental data when θ_z ($\geq 7^\circ, \geq 6^\circ$) respectively. The stability of the results against the variation of θ_z , wherever it is possible, from nearly 0° to 10° is achieved in five of the allowed models (the remaining ones except **N5**). In fact, the stability is also achieved in two of the disallowed models, namely **I2** and **I4**.

As to the Dirac-phase, we found the solution in many cases, especially for the allowed models, to depend sensitively on its value, so that any deviation from it violates the experimental constraints. This point was not addressed in [13], and we illustrate it in figure (7), corresponding to case **I1** of the two-vanishing minors texture. Here, for the choice $\theta_x = 34^\circ$, $\theta_y = 42^\circ$ and $\theta_z = 5^\circ$, we vary δ and find that satisfying the condition (13) singles out a nearly right angle for δ . This offers a good way for selecting the appropriate Dirac phase δ which we adopted in our present work.

In all the successful models, the non oscillation parameters $\langle m \rangle_e$, $\langle m \rangle_{ee}$ and Σ are consistent with the bounds given in eq. (12). In addition, $\langle m \rangle_e$, $\langle m \rangle_{ee}$ and m_3 have the same order of magnitude. The mass sum parameter is always constrained to be $\Sigma \leq 0.242$ eV which is safe with the cosmological bound in eq. (12).

Concluding remarks are in order. First, for all patterns the leading terms in the expansion of the angles (ρ, σ) in powers of $(\sin(\theta_z))$ are either δ or $\frac{\delta}{2} \pmod{\frac{\pi}{2}}$. Second, the models **N1**, **N2**, **N5**, **I1** and **I3** do not have room for the atmospheric mixing angle to be maximal ($\frac{\pi}{4}$), otherwise the parameter R_ν would become too large. Third, all models can be generated in the frame work of flavour Abelian discrete symmetry, and additional scalar fields with appropriate transformation properties, implemented in seesaw schemes.

Acknowledgements

Both authors would like to thank L. Lavoura for drawing our attention to his work. One of the authors, E. I. Lashin would like to thank both of A. Smirnov and S. Petcov for useful discussions. Part of this work was done within the associate scheme of ICTP.

References

- [1] Y. Fukuda *et al.*, Phys. Lett. B **436**, 33 (1998); Phys. Rev. Lett. **81**, 1562 (1998). For a review, see: C.K. Jung, C. McGrew, T. Kajita, and T. Mann, Ann. Rev. Nucl. Part. Sci. **51**, 451 (2001).
- [2] S. M. Bilenky, and B. Pontecorvo, Phys. Rep **41**, 225 (1978);
S. M. Bilenky and S. T. Petcov, Rev. Mod. Phys. **59**, 671, (1987)
- [3] Particle Data Group, K. Hagiwara *et al.*, Phys. Rev. D **66**, 010001 (2002).
- [4] SNO Collaboration, Q.R. Ahmad *et al.*, Phys. Rev. Lett. **89**, 011301 (2002); Phys. Rev. Lett. **89**, 011302 (2002).
- [5] KamLAND Collaboration, K. Eguchi *et al.*, Phys. Rev. Lett. **90**, 021802 (2003).
- [6] K2K Collaboration, M.H. Ahn *et al.*, Phys. Rev. Lett. **90**, 041801 (2003).
- [7] CHOOZ Collaboration, M. Apollonio *et al.*, Phys. Lett. B **420**, 397 (1998); Palo Verde Collaboration, F. Boehm *et al.*, Phys. Rev. Lett. **84**, 3764 (2000).
- [8] P.H. Frampton, S.L. Glashow, and D. Marfatia, Phys. Lett. B **536**, 79 (2002).
- [9] Z.Z. Xing; Phys. Lett. B **530** (2002), 159-166
- [10] Z.Z. Xing; Phys. Rev. D **69**, 013006 (2004)
- [11] E. Ma; Phys. Rev. D **71**, 111301 (2005)
- [12] S.-L. Chen, M. Frigerio and E. Ma; Nucl. Phys. B **724**, 423 (2005)
- [13] L. Lavoura; Phys. Lett. B **609**, 317 (2005)
- [14] H. A. Alhendi, E. I. Lashin and A. A. Mudlej, Phys. Rev. D **77**, 013009 (2008); hep-ph/0708.2007
- [15] G. L. Fogli *et al.*, Prog. Part. Nucl. Phys. **57**, 742 (2006)
- [16] W. Grimus, A.S. Joshipura, L. Lavoura and M. Tanimoto, Eur. Phys. J. C **36**, 227 (2004)